Applied Catalysis B: Environmental 125 (2012) 28–34

Contents lists available at SciVerse ScienceDirect

Applied Catalysis B: Environmental

journal homepage: www.elsevier.com/locate/apcatb

Photocatalytic removal of 2,4-dichlorophenoxyacetic acid by using sol–gel synthesized nanocrystalline and commercial TiO_2: Operational parameters optimization and toxicity studies

E.I. Seck*, J.M. Doña-Rodríguez*, C. Fernández-Rodríguez, O.M. González-Díaz, J. Araña, J. Pérez-Peña

Grupo de Fotocatálisis y Espectroscopía Aplicada al Medioambiente-FEAM (Unidad Asociada al Instituto de Ciencia de Materiales de Sevilla, C.S.I.C.), CIDIA-Depto. de Química, Edificio del Parque Científico Tecnológico, Universidad De Las Palmas De Gran Canaria, Campus Universitario de Tafira, 35017, Las Palmas, Spain

ARTICLE INFO

Article history:
Received 7 February 2012
Received in revised form 13 May 2012
Accepted 18 May 2012
Available online 30 May 2012

Keywords:
2,4-Dichlorophenoxyacetic acid
Photocatalysis
ECT-1023t
Vibrio fischeri
H_2O_2
FTIR

ABSTRACT

A comparative study of the photoefficiency of two different TiO_2 catalysts in the elimination, mineralization and detoxification of waters containing herbicide 2,4-dichlorophenoxyacetic acid (2,4-D) and toxic intermediates was performed at laboratory scale. Commercial TiO_2 (Degussa (Evonik) P25) and TiO_2 synthesized by citrate sol–gel method (ECT-1023t) were selected as photocatalysts. Adsorption studies, kinetic analysis and an analysis of the effect of adding oxidizing agents (H_2O_2 and $S_2O_8^{2-}$) were carried out for both catalysts. The toxic effect of photocatalytic treatment at different reaction times was determined by marine bacteria *Vibrio fischeri* bioassay. The toxic effect on this organism of the main degradation intermediate 2,4-dichlorophenol (2,4-DCP) was higher than for the initial herbicide. The optimal operational variables to eliminate the herbicide and toxic intermediates were established for both catalysts. The most effective removal of 2,4-D and toxic intermediate 2,4-DCP was achieved using ECT-1023t as catalyst at pH 3 and pH 5. The inhibitory effect on *V. fischeri* growth in water containing 2,4-D after 2 h of photocatalytic treatment was negligible when using ECT-1023t as catalyst. Longer times were necessary to obtain similar results when using P25 as catalyst. The addition of H_2O_2 significantly enhanced the degradation and mineralization rate, with different optimal H_2O_2 concentrations for the tested catalysts. When using H_2O_2 as oxidizing agent, toxicity on *V. fischeri* was eliminated before 1 h of photodegradation treatment with both photocatalysts.

1. Introduction

The availability of clean water is of particular importance for developing countries in both rural villages and rapidly growing metropolitan areas which commonly lack adequate infrastructure for water and wastewater treatment. The agricultural chemical 2,4-dichlorophenoxyacetic acid (2,4-D) is extensively used for the control of dicotyledonous weeds in cereal crops [1,2]. It has been used for weed control on wheat, barley, oats, rye, rice, maize and sorghum. 2,4-D is considered to be potentially dangerous to both animals and humans and is a well-known endocrine disruptor [3]. Its biodegradability is extremely low and it has been detected as a major contaminant in effluents from both subterranean and superficial waters [4,5]. Though this compound has been banned in most developed countries, it is unfortunately still the most widely used herbicide in West Africa, especially in Senegal where agriculture amounts to approximately 20% of the gross domestic product (GDP). Photocatalysis, a process based on absorption of energy (visible or UV light) by a solid (a semiconductor), is a promising method for the elimination of organic pollutants in water [6,7]. The photocatalytic properties of the semiconductors are based on their electronic structure which is characterized by a filled valence band and an empty conduction band. When they are illuminated with energy greater than their band gap energy, E_g, electrons are promoted from the valence band to the conduction band leaving a hole and pairs (e^-/h^+) are produced. These species can recombine in the bulk of the semiconductor and dissipate the input energy as heat, or they can migrate to the surface of the semiconductor's particles and react with adsorbed electron donors or electron acceptors. The photogenerated holes act as powerful oxidants and the electrons as powerful reducing agents and initiate a wide range of chemical redox reactions, which can lead to partial or total destruction of a great variety of organic pollutants [8]. This technology displays certain advantages over other processes, but it is limited to low concentrations of pollutants. Titanium dioxide is the most commonly used photocatalyst due to its high photoactivity, non-toxic nature, large band-gap and stability [9]. Among the various kinds of TiO_2 that are commercially available, Degussa (Evonik) P25 is routinely used as a benchmarking material due to its satisfactory activity

* Corresponding authors. Tel.: +34 928457301; fax: +34 928457397.
E-mail addresses: seck36@yahoo.fr (E.I. Seck), jdona@dqui.ulpgc.es (J.M. Doña-Rodríguez).

0926-3373/$ – see front matter © 2012 Elsevier B.V. All rights reserved.
http://dx.doi.org/10.1016/j.apcatb.2012.05.028

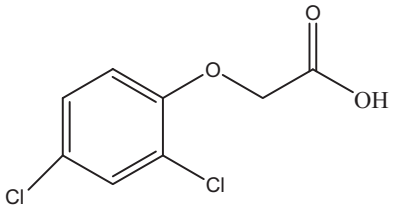

Scheme 1. Chemical structure of 2,4-dichlorophenoxyacetic acid.

for most organic contaminants. However, P25 has certain limitations for up-scaling applications due to slow settling at optimal pH values of photocatalytic performance and its moderate photoactivity for the removal of toxic phenolic compounds. In a previous study, the synthesis of a highly photoactive TiO_2 (ECT-1023t) to remove phenolic compounds from water was successfully achieved by our group [10]. This material was synthesized by sol–gel hydrolysis precipitation of titanium butoxide. Subsequently, amorphous sample from the sol–gel process was sieved and calcined at 1023 K. High anatase–rutile ratio TiO_2 particles with larger average particle size than P25 were obtained by this method. Several studies have demonstrated that the most efficient TiO_2 photocatalysts in the degradation of phenol are those with large particle size, high crystallinity and high anatase phase content [11,12]. The increased photoefficiency of ECT-1023t sample on phenol removal can be attributed to the highest rate of OH radical formation on anatase particles calcined at high temperature [13].

The aim behind this work is to compare the photocatalytic degradation and mineralization of 2,4-D and toxic phenolic intermediates using Degussa (Evonik) P25 and ECT-1023t in order to test the photoefficiency of the novel home-made catalyst with other types of pollutants. Special attention was given to analyze the efficiency of both photocatalysts in eliminating the toxicity of water containing the herbicide and toxic intermediates. With this in mind, a bacterial assay was carried out based on the bioluminescence reduction of the marine bacterium *Vibrio fischeri*, using a Microtox analyser.

2. Experimental

2.1. Materials and reagents

Analytical reagent grade 2,4-D (see Scheme 1) with 97% purity was obtained from Aldrich. Titanium dioxide (Degussa (Evonik) P25) was predominantly anatase (80% anatase and 20% rutile) with a surface area of 52 $m^2\,g^{-1}$, a 3.18 eV band gap and an average particle size of 27 nm. The TiO_2 ECT-1023t (89–94% anatase and 11–6% rutile, with surface area 18.3 $m^2\,g^{-1}$, a 2.97 eV band gap and average particle size 71 nm) was prepared by sol gel method and calcined at 1023 K. The synthesis and characterization of this photocatalyst were reported in a previous paper [10]. The real particle size distribution of each suspension, measured under experimental conditions using dynamic light scattering technique, showed a particle size of 3 μm and 39 μm for P25 and ECT-1023t, respectively (Fig. 9).

2.2. Irradiation and adsorption experiments

All irradiation experiments were carried out in a Pyrex cylindrical reactor of 250 cm^3. Chemisorption of organic compounds on the catalyst surface was favored by stirring and air-bubbling (400 mL/min) at room temperature for 30 min in the dark before UV light exposure. A 60 W Solarium Philips HB175 equipped with four 15 W Philips CLEO fluorescent tubes with emission spectrum from 300 to 400 nm (maximum around 365 nm) (9 mW/cm^2) was used as light source. Prior to photocatalytic experiments, an adsorption study of 2,4-D on the catalyst surface was carried out in the dark by mixing aqueous solution of a fixed concentration of 2,4-D with 1 $g\,L^{-1}$ of catalyst. The mixture containing 2,4-D and TiO_2 powder was continuously stirred. Aliquots were withdrawn at 1 h and the change in 2,4-D concentration was measured. The extent of equilibrium adsorption was determined from the decrease in 2,4-D concentration.

2.3. Product analysis

Samples were withdrawn from the reactor during the degradation experiments at different reaction times and filtered through a 0.45 μm pore size membrane PTFE filter. The 2,4-D concentration in solution was determined by high-performance liquid chromatography (HPLC). A Varian Chromatograph equipped with a DAD (diode array detector) was used. The wavelength was established at 214 nm. The remaining concentrations of the compounds at different reaction times were measured using a Supelco Discovery C18 column (25 cm × 4.6 mm ID, particle size of 5 μm), with mobile phase consisting of 70% methanol and 30% phosphoric acid buffer at pH 2.3. H_2O_2 concentration was monitored by HPLC at 210 nm with 20% acetonitrile and 80% water as mobile phase. The extent of mineralization was determined using a total organic carbon (TOC) analyzer (TOC-VCSH, Shimadzu). A Dionex ion chromatograph was used to determine chloride concentrations.

For the Fourier transform infrared (FTIR) experiments, a spectrophotometer model RS/1 (UNI-CAM) was used for FTIR spectra. Intervals of 4000–1000 cm^{-1}, a resolution of 2 cm^{-1} and forward–reverse moving mirror speeds of 10 and 6.2 kHz, respectively, were used. These analyses were performed by placing films of the catalysts between two CaF_2 windows. In 2,4-D interaction studies, the catalysts (P25 and ECT-1023t, respectively) remained in contact with the solution of 2,4-D at pH 3 during 24 h. After this, the catalyst was then filtered and the water evaporated at room temperature.

2.4. Toxicity analysis

2.4.1. Vibrio fischeri bioassay

The toxicity of the initial 2,4-D solution and of several irradiated samples, collected at different time intervals from the slurry system, was examined by a Microtox chronic toxicity test. This test uses the marine bioluminescent bacteria, *V. fischeri*, as test organism. Freeze-dried bacteria, reconstitution solution, diluent (2% NaCl) and an adjustment solution (non-toxic 20% sodium chloride) were obtained from Aboatox. Samples were analyzed by the Microtox® bioassay according to the screening procedure. Briefly, three aliquots of each sample were tested in medium containing 2% NaCl and luminescence was recorded after 15 min of incubation at 15 °C. The inhibition of the luminescence, compared to a toxic-free control (negative control) gives the percentage of inhibition.

3. Results and Discussions

3.1. Adsorption studies using the Freundlich isotherm model

A comparative adsorption study of 2,4-D onto Degussa (Evonik) P25 and ECT-1023t (1 $g\,L^{-1}$) was performed at different initial 2,4-D concentrations from 0.1 to 1 mM for 1 h.

The Freundlich isotherm [14] Eq. (1) is an empirical equation employed to describe heterogeneous systems:

$$\ln q_e = \ln K_F + \frac{1}{n}\ln C_e \quad (1)$$

Table 1
Freundlich adsorption isotherm parameters for 2,4-D on Degussa (Evonik) P25 and ECT-1023t (1 g L^{-1}, pH 3).

	Degussa P25	ECT-1023t
K_F (ppm^{-1})	0.1160	0.0010
n	1.3314	0.6596
R^2	0.9913	0.9805

where K_F and n are constants, with K_F being the adsorption capacity of the sorbent and n indicating how favorable the adsorption process is. Values of $n > 1$ represent favorable adsorption condition [15,16]. Values of K_F and n for both photocatalysts were calculated from the intercept and slope of the experimental data (Fig. 1) fitted to Eq. (1) and listed in Table 1. Favorable adsorption was observed when using P25 as photocatalyst ($n = 1.3314$, $R^2 > 0.99$) though this was not the case for ECT-1023t ($n = 0.6596$, $R^2 = 0.9805$).

3.2. FTIR studies

The FTIR spectra of P25 and ECT-1023t after equilibrium adsorption with 2,4-D in the dark at pH 3 (pH of optimal adsorption) were compared with the pure 2,4-D. As can be seen in Fig. 2, the FTIR spectra of 2,4-D shows the characteristic C=O band of carboxylic acid groups at 1700 cm^{-1}. The two aromatic C=C bands of the benzene ring are observed as a very weak band at 1583 cm^{-1} and a more intense band at 1481 cm^{-1}. The CH_2 band can be observed at 1448 cm^{-1} and the C—O band of the carboxylic functional group at 1240 cm^{-1}. Two different bands associated with the R—O—CH_2 (where R is the phenyl group) can be observed at 1100 cm^{-1} and 1308 cm^{-1}. FTIR spectra of adsorbed 2,4-D on P25 and ECT-1023t revealed the total absence of the characteristic band of the acid (1700 cm^{-1}) and the appearance of bands corresponding to the carboxylate anion, COO^-, at 1590 cm^{-1} and 1430 cm^{-1} (in the case of P25 it seems that two different types of carboxylates appeared, one at 1590 cm^{-1}, as occurred with ECT-1023t, and another at 1618 cm^{-1}). The disappearance of the R—O—CH_2 bands in the case of both catalysts can also be observed.

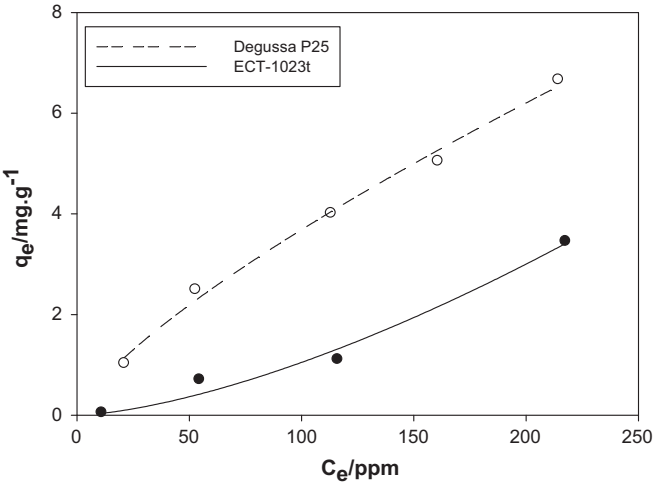

Fig. 1. Freundlich isotherm adsorption of 2,4-D on Degussa (Evonik) P25 and ECT-1023t (1 g L^{-1}, pH 3).

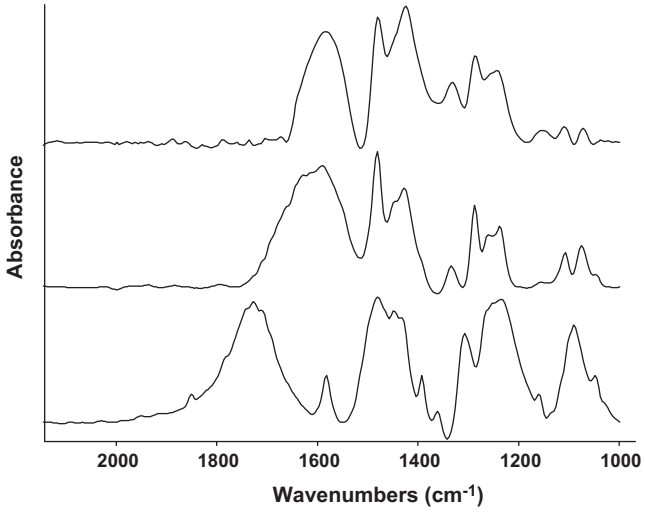

Fig. 2. FTIR spectra from interaction of 2,4-D with the two catalysts at pH 3. Reference spectrum 2,4-D.

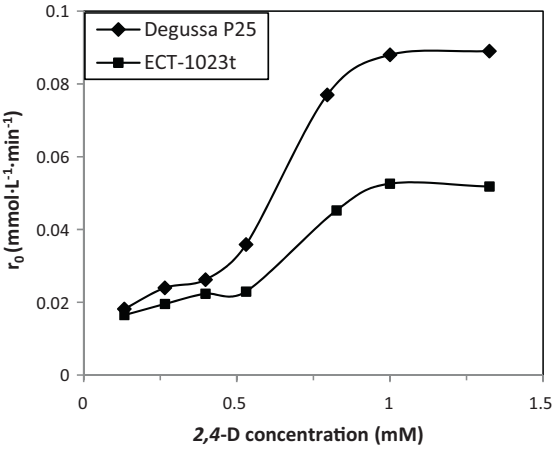

Fig. 3. Initial rate of degradation vs. initial concentration of 2,4-D for the two catalysts at pH 3.

The interaction between 2,4-D with P25 and ECT-1023t confirmed that its adsorption on both catalysts at pH 3 occurred essentially through carboxylate anion formation and the weakening or breaking of R—O—CH_2 bands. These results confirmed that the mechanism of the oxidation of 2,4-D via holes and to a lesser extent OH radicals (leading to the formation of the main intermediate, the 2,4-dichlorophenol (2,4-DCP) [2].

The greater adsorption of 2,4-D on P25 (surface area 52 m^2 g^{-1}) at pH 3 in comparison to ECT-1023t (surface area 18 m^2 g^{-1}) can be explained in terms of the difference in surface area.

3.3. Effect of initial 2,4-D concentration

A comparative effect of initial 2,4-D concentration on the initial degradation rate at pH 3 was studied from 0.1325 to 1.325 mM using Degussa (Evonik) P25 and ECT-1023t as catalyst (1 g L^{-1}). The results can be seen in Fig. 3. It can be seen that the degradation rate increases with initial concentration of 2,4-D up to 1 mM (more rapidly with Degussa (Evonik) P25 than with ECT-1023t), following a pseudo-first-order kinetic, whereas for concentrations >1 mM the reaction rate is maximum and follows an apparent zero order kinetic. The initial degradation rate is 0.088 mmol L^{-1} min^{-1} and 0.053 mmol l^{-1} min^{-1} for P25 and ECT-1023t, respectively. This double behavior is in accordance with the Langmuir–Hinshelwood mechanism. Considering this behavior, it can be suggested that the ECT-1023t saturation rate is reached faster than is the case for Degussa (Evonik) P25, probably due to the difference in surface area between the two catalysts (52 m^2 g^{-1} and 18 m^2 g^{-1} for Degussa (Evonik) P25 and ECT-1023t, respectively).

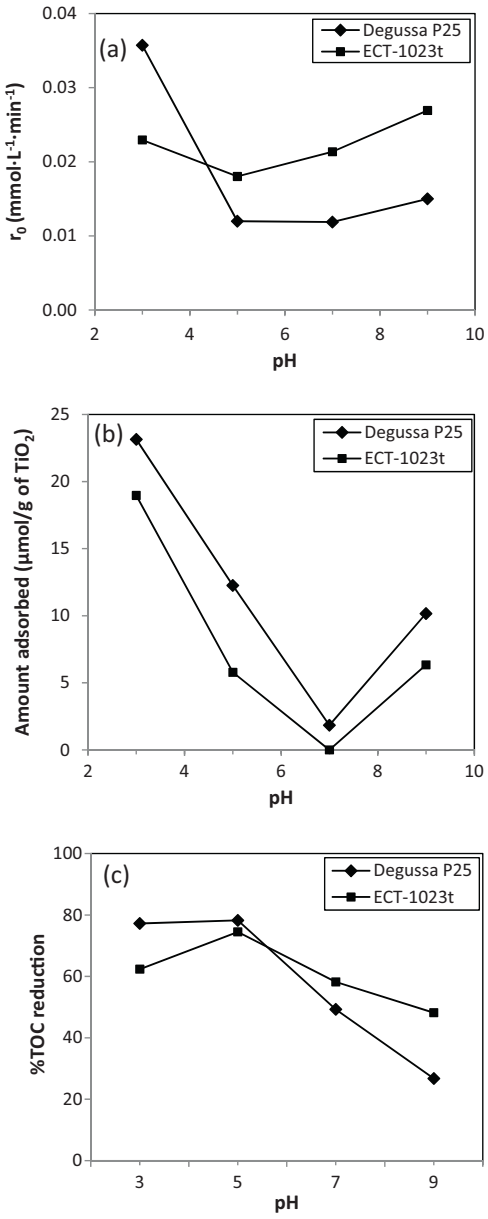

Fig. 4. (a) Initial rate of degradation of 2,4-D vs. pH. (b) Moles of 2,4-D adsorbed onto the two catalysts. (c) Percentage of TOC reduction vs. pH for the two catalysts.

3.4. Operational parameters

3.4.1. pH effect

The photocatalytic degradation of 2,4-D with Degussa (Evonik) P25 and ECT-1023t at different reaction pH values between 3 and 9 was studied. In Fig. 4a, the initial rate of 2,4-D photodegradation (r_0) with both photocatalysts as a function of reaction pH value is depicted. A gradual decrease of r_0 with increasing pH value occurs with P25, while with ECT-1023t a different behavior is noticed: an almost constant value of r_0 with increasing pH value. However, from dark adsorption data (Fig. 4b) a decrease is observed for both photocatalysts of the mass of 2,4-D adsorbed with increasing initial pH value from 3 to 7 and then a slight increase from 7 to 9. However, the degree of adsorption of 2,4-D on P25 is slightly more important than in the case of ECT-1023t particles due probably to its high surface area compared to the home made catalyst. It seems that above a value of pH > pK_a of 2,4-D (pK_a = 2.9) [17] dark adsorption decreases. This trend agrees with the pH effects upon acid–base equilibrium on the catalyst surface and species in solution. Such equilibrium leads to a lack of positive surface charges on the catalyst and an increase of negatively charged species concentration in solution with increasing pH, enlarging the electrostatic repulsion between acidic substrates and TiO_2 surface. From these observations, it seems clear that in order to degrade 2,4-D with P25 a previous adsorption step must occur, which is not necessary with ECT-1023t. For this reason, the formation rate of mobile hydroxyl radicals seem to more higher on ETC-1023t than on P25. TOC reduction (Fig. 4c) is more important at pH 5 and similar for both catalysts because the main photodegraded intermediate of 2,4-D (2,4-DCP) is photodegraded faster at pH 5 than at pH 3, as can be seen in Table 2 [18]. However, from an economic point of view, at natural pH of real waters (pH 6–8) without any additives, the ECT-1023t would seem to perform better than P25 in terms of both degradation and mineralization of 2,4-D.

Table 2
Initial rates (mmol L^{-1} min^{-1}) of photocatalytic degradation of 2,4-dichlorophenol 0.53 mM at pH 3 and 5, for Degussa (Evonik) P25 and ECT-1023t suspensions.

	pH 3	pH 5
r_0 (Degussa P25)	0.0101	0.0128
r_0 (ECT-1023t)	0.0208	0.0238

3.4.2. Catalyst amount

The reaction rate as a function of the amount of catalyst is an important operational parameter for up-scaling the photocatalytic treatment [19,20]. The influence of the photocatalyst concentration on the degradation kinetics and mineralization of 2,4-D was investigated by varying from 0.5 to 4 g L^{-1} the concentrations of Degussa (Evonik) P25 and ECT-1023t, respectively. It can be seen from Fig. 5 that when using P25 the addition of catalyst markedly improves the initial rate of degradation and mineralization of the 2,4-D. However, the effect of increasing the concentrations above

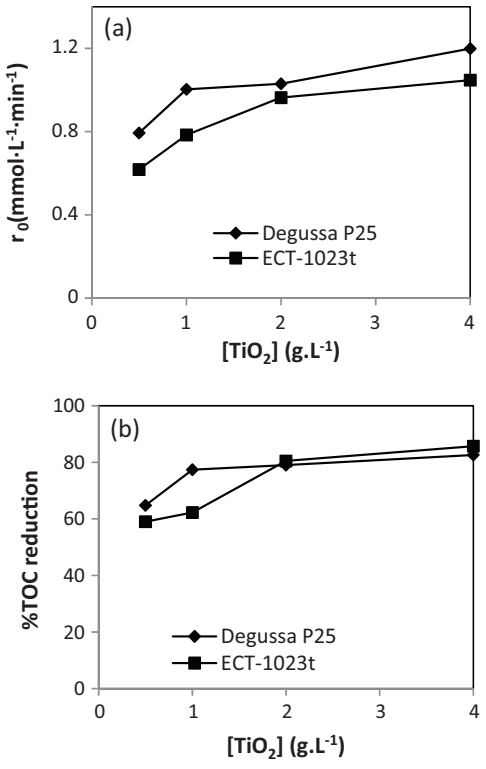

Fig. 5. (a) Initial degradation rate of 2,4-D vs. catalyst loading (0.5–4 g L^{-1}, pH 3). (b) Percentage of TOC reduction vs. catalyst loading (0.5–4 g L^{-1}, pH 3).

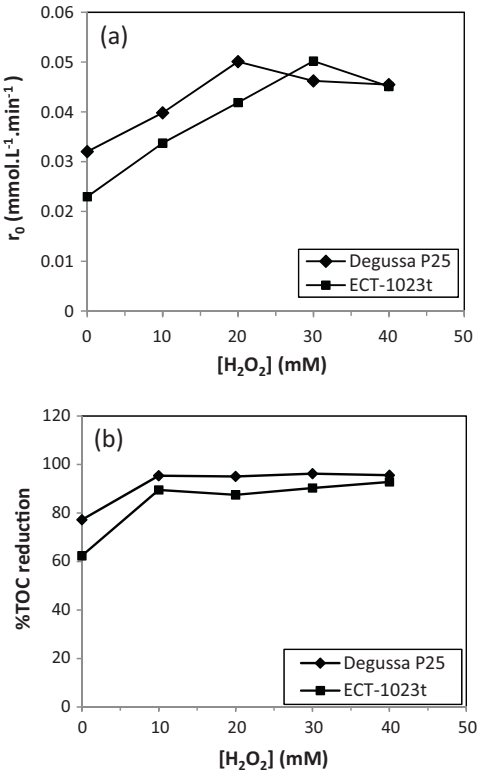

Fig. 6. (a) Initial degradation rate of 2,4-D vs. H_2O_2 concentration at pH 3. (b) Percentage of TOC reduction vs. H_2O_2 concentration at pH 3.

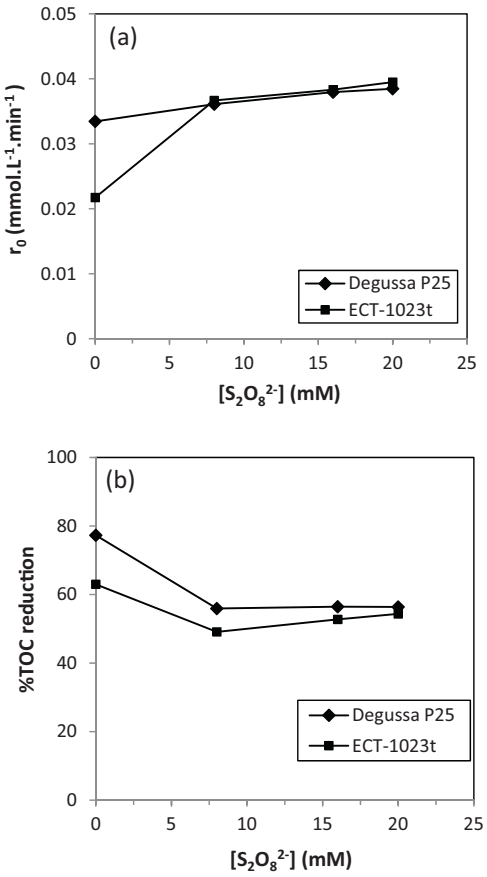

Fig. 7. (a) Initial degradation rate of 2,4-D vs. $S_2O_8^{2-}$ concentration at pH 3. (b) Percentage of TOC reduction vs. $S_2O_8^{2-}$ concentration at pH 3.

1 g L^{-1} was negligible. A similar trend was reported for the photocatalytic degradation of phenoxy acetic acid (PAA) with P25, UV100 and PC500 [21]. The same behavior is observed with ECT-1023t, although 2 g L^{-1} of catalyst was required to attain the same initial rate of degradation and exceed the percentage of mineralization achieved when using P25 as catalyst. The surface area of P25 and ECT-1023t was 52 m^2 g^{-1} and 18 m^2 g^{-1}, respectively. Hence, if surface area is considered, the efficiency of ECT-1023t for the removal of 2,4-D and photogenerated intermediates was higher than P25 at all catalyst loading tested

3.5. Effect of adding oxidizing agents

3.5.1. Effect of adding H_2O_2

Addition of H_2O_2 to TiO_2 suspensions is a well-known procedure and in many cases leads to an increase in the rate of photocatalytic oxidation [22,23]. Its beneficial effect can be explained by a prevention of electron/hole recombination and additional •OH production. The inhibition effect could be explained by TiO_2 surface modification by H_2O_2 adsorption, scavenging photogenerated holes and reacting with hydroxyl radicals. The optimum concentration of H_2O_2 depends on the type of catalyst and also on the type and concentration of the tested pollutants. In order to investigate the effect of H_2O_2 addition, experiments were conducted by varying the initial H_2O_2 concentration in the range 10–40 mM.

From Fig. 6a, it can be observed that the addition of H_2O_2 improves the photocatalytic degradation of 2,4-D when using both suspended catalysts. For instance, maximum initial photodegradation rate of 2,4-D was 0.05 mol L^{-1} min^{-1} in the presence of 20 mM H_2O_2 and 0.032 mol L^{-1} min^{-1} without H_2O_2 when using P25 as photocatalyst. The same photodegradation rate was achieved with ECT-1023t when adding 30 mM of H_2O_2.

TOC reduction was considerably enhanced in the presence of H_2O_2. The maximum value for both catalysts was attained with the addition of only 10 mM of H_2O_2 (Fig. 6b). TOC reduction for P25 after 2 h was 95.4% and 77.2% with and without H_2O_2, respectively. In the case of ECT-1023t, the respective figures with and without H_2O_2 were 89.54% and 62.37%. This result for both catalysts can be explained by the fact that addition of H_2O_2 considerably improves the photodegradation rate of the main intermediate 2,4-DCP, as can be seen in Fig. 6a and b.

When the synthetic solution was irradiated in the presence of H_2O_2 without catalyst, 2,4-D degradation and mineralization were negligible. The same experiment was repeated in the dark and resulted in negligible 2,4-D degradation and mineralization.

3.5.2. Effect of adding $S_2O_8^{2-}$

Peroxodisulfate can be a beneficial oxidizing agent in photocatalytic detoxification [24,25] because $SO_4^{\bullet-}$ (E = 2.6 eV) are formed from the oxidant compound by reaction with the photogenerated semiconductor electrons (Eq. (2)). However, the initial photodegradation rate of compounds might decrease due to SO_4^{2-} adsorption onto TiO_2 surface [26,27]. The effect of $S_2O_8^{2-}$ addition was studied by varying the initial concentration from 8 to 20 mM in the presence of the two catalysts (Fig. 7a). The addition of peroxodisulfate improved slightly the 2,4-D removal from water using ECT-1023t as catalysts. However, no significant differences in the improvement of the 2,4-D photodegradation rate were obtained when using P25. The same experiment was repeated in the dark showing negligible 2,4-D degradation. TOC reduction (Fig. 7b) was not affected by the addition, with only a slight decrease observed as a result of the inhibitory effect of the peroxodisulfate on the degradation of the main intermediate. A competitive adsorption between the 2,4-D and the SO_4^{2-} anions and between the 2,4-D intermediates and

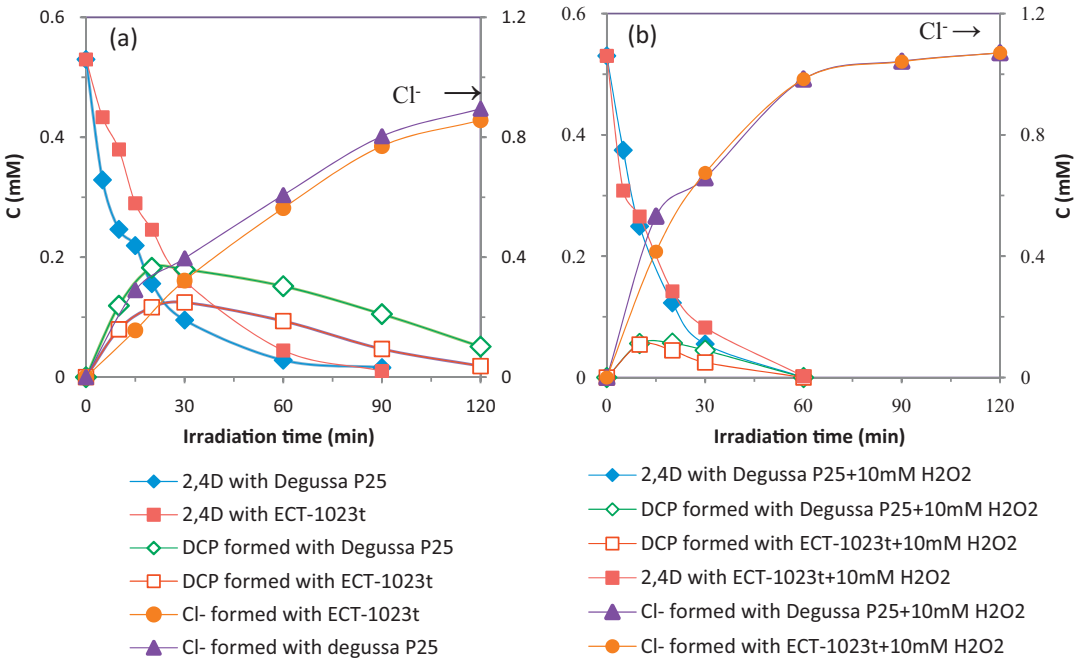

Fig. 8. (a) Time-course of 2,4-D, chloride ions and 2,4-DCP formed without H_2O_2 for the two catalysts. (b) Time-course of 2,4-D, chloride ions and 2,4-DCP formed with H_2O_2 for the two catalysts at pH 3.

the SO_4^{2-}, where the ions should modify the superficial properties of TiO_2 can be envisaged to explain these behaviors.

$$S_2O_8^{2-} + e_{CB}^- \rightarrow SO_4^{2-} + SO_4^{\bullet -} \quad (2)$$

3.6. Evolution of chloride ions and 2,4-DCP formed during photocatalytic degradation of 2,4-D with Degussa (Evonik) P25 and ECT-1023t

The main intermediate identified by HPLC with both photocatalysts was 2,4-DCP which is more toxic than the parent 2,4-D. The elimination of 2,4-DCP was more rapid when using ECT-1023t than when using P25 at pH 3 and pH 5 (Table 2). The formation of this intermediate can be explained by considering the attack of an •OH radical on the alkyl chain of the molecule [2]. Without H_2O_2, chloride ions in solution attained a concentration value of 31.78 ppm with P25 and 30.4 ppm with ECT-1023t after 2 h of irradiation, which is 86% of the initial chlorine as 2,4-D for P25 and 83% for ECT-1023t (Fig. 8a). Using H_2O_2, the stoichiometric concentration of chloride in solution was attained before 1 h of degradation with both photocatalysts, with the main intermediate 2,4-DCP being completely removed in the same time period (Fig. 8b).

3.7. Microtox bioassay toxicity on Vibrio fischeri

An important photocatalytic process parameter is the evolution of toxicity. The acute bioluminescence inhibition assay using the marine bacterium *V. fischeri* as the test organism is a widely used short-term toxicity test. We chose the standardized method to compare the detoxification process using Degussa (Evonik) P25 and ECT-1023t.

Table 3 shows the results of the toxicity assays of different reaction times by using 1 g L^{-1} of catalyst at pH 3 and pH 5. It was observed that the inhibitory effect of samples on bacteria bioluminescence increased after 1 h of treatment. This effect is due to the appearance of intermediates such as 2,4-DCP, which is considerably more toxic than the parental pesticide. However, toxicity began to decrease after 2 h until its full elimination after 3–4 h. Interestingly, photocatalytic treatment when using ECT-1023t as catalyst resulted in faster detoxification than the commercial catalyst at pH 3, with the difference in the detoxification rate for the two catalysts rising even higher at pH 5. This is an indicator of the higher degradation rate of the toxic intermediates when using ECT-1023t (Table 2). It should also be mentioned that when H_2O_2 was used as oxidizing agent, toxicity was eliminated before 1 h of photodegradation for both catalysts because of the faster elimination of 2,4-DCP in the presence of H_2O_2. Toxicity evolution correlates perfectly with dichlorophenol elimination. The intermediates formed during the oxidation of 2,4-DCP are less toxic than the parental compound [28].

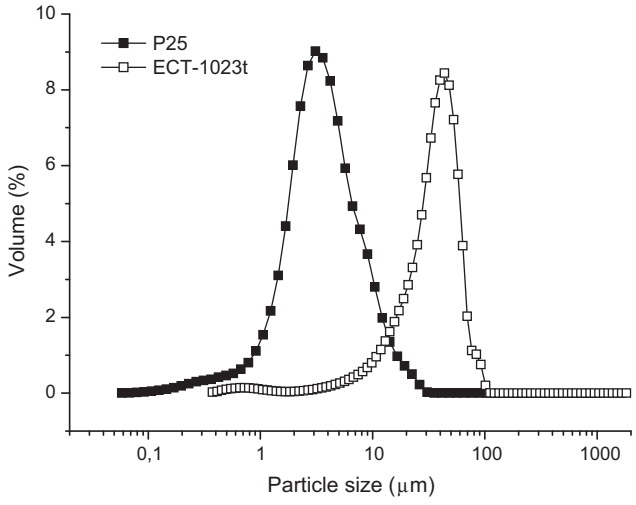

Fig. 9. Particle size distribution of P25 and ECT-1023t.

Table 3
Changes in the % of inhibition of bioluminescence of *Vibrio fischeri* at different irradiation times when using Degussa (Evonik) P25 and ECT-1023t (C_0 = 0.53 mM catalyst amount 1 g L^{-1}).

Sample	Degussa P25, pH 3	ECT-1023t, pH 3	Degussa P25, pH 5	ECT-1023t, pH 5	Degussa P25 + 10 mM H_2O_2, pH 3	ECT-1023t +10 mM H_2O_2, pH 3	Degussa P25 + 10 mM H_2O_2, pH 5	ECT-1023t +10 mM H_2O_2, pH 5
0 min	53.75	48.21	53.75	53.75	53.75	53.75	53.75	53.75
60 min	98.46	99.90	86.32	99.70	OFF curve	OFF curve	52.99 (15 min)	45.47 (15 min)
120 min	93.02	99.59	42.94	20.82	OFF curve	OFF curve	52.77 (30 min)	36.19 (30 min)
180 min	1.291	OFF curve	9.175	OFF curve	OFF curve	OFF curve	2.332 (45 min)	OFF curve (45 min)
240 min	OFF curve	OFF curve	OFF curve	OFF curve	OFF curve	OFF curve	OFF curve (60 min)	OFF curve (60 min)

4. Conclusion

It can be concluded from the results of the present study that the use of the homemade TiO_2 degraded the 2,4-D herbicide and its toxic intermediates more efficiently than the Degussa (Evonik) P25 at pH values of fresh water (from 5 to 9). Indeed, ECT1023t eliminated more rapidly the main intermediate of this herbicide which is much more toxic than the parental pesticide. This result is very interesting since it is very difficult to find 2,4-D in appreciable concentrations in the environment as it naturally degrades to the more recalcitrant and more toxic 2,4-DCP. Another beneficial parameter from the use of ECT-1023t is that because this catalyst sediments more easily and faster than P25 because of its big aggregates in comparison with P25 (Fig. 9). For this reason it is relatively easy to recover after treatment and can therefore be used in higher concentrations. Addition of the environmentally friendly oxidizing agent, hydrogen peroxide, led to rapid elimination of the 2,4-DCP. Toxicity was thus eliminated in a very short time. In conclusion, this study highlights that assessment of the photocatalytic efficiency of novel catalysts should include not only measurement of the degradation rate of specific substrates, but also evaluation of the toxic remediation of the treatment.

Acknowledgments

We are grateful for the funding of the European Commission through the Clean Water Project which is a Collaborative Project (grant agreement no. 227017) co-funded by the Research DG of the European Commission within the joint RTD activities of the Environment and NMP Thematic Priorities. Furthermore, we wish to thank the Spanish Ministry of Science and Innovation for their financial support through the Project CTQ2008-05961-C02-02 and the Spanish Ministry of Foreign Affairs and Cooperation for their financial support to Mr. E.I. Seck.

References

[1] "Catalogo Oficial de Plaguicidas 2004 de la Comision Intersecretarial para el Control del Proceso y Uso de Plaguicidas, Fertilizantes y Sustancias Toxicas (CICOPLAFEST)", Mexico, 2004.
[2] M. Trillas, J. Peral, X. Doménech, Applied Catalysis B: Environmental 5 (1995) 377.
[3] T. Colborn, F.S. Vom Saal, A.M. Soto, Environmental Impact Assessment Review 14 (1993) 469–489.
[4] E. Brillas, J.C. Calpe, P.L. Cabot, Applied Catalysis B: Environmental 46 (1986) 381.
[5] D.G. Hoover, G.E. Borgonov, S.H. Jones, M. Alexander, Applied and Environment Microbiology 51 (1986) 226.
[6] M.A. Fox, M.T. Dulay, Chemical Reviews 93 (1993) 341–357.
[7] A. Fujishima, T.N. Roa, D.A. Tryk, Journal of Photochemistry and Photobiology C: Photochemistry Review 1 (2000) 1–21.
[8] M.R. Hoffmann, S.T. Martin, W. Choi, D.W. Bahnemann, Chemical Reviews 95 (1995) 69–96.
[9] U.I. Gaya, A.H. Abdullaha, Journal of Photochemistry and Photobiology C: Photochemistry Reviews 9 (2008) 1–12.
[10] J. Araña, J.M. Doña-Rodríguez, D. Portillo-Carrizo, C. Fernández-Rodríguez, J. Pérez-Peña, O. González Díaz, J.A. Navío, M. Macías, Applied Catalysis B: Environmental 100 (1–2) (2010) 346–354.
[11] A.G. Agrios, Pierre Pichat, Journal of Photochemistry and Photobiology A: Chemistry 180 (2006) 130–135.
[12] J. Ryu, W.Y. Choi, Environmental Science and Technology 42 (2008) 294–300.
[13] B. Tryba, M. Toyoda, A.W. Morawski, R. Nonaka, M. Inagaki, Applied Catalysis B: Environmental 71 (2007) 163–168.
[14] H. Freundlich, Zeitschrift für Physikalische Chemie 57 (1906) 384–470.
[15] R.E. Treybal, Mass Transfer Operations, second ed., McGraw Hill, New York, 1968.
[16] Y.S. Ho, G. McKay, Chemical Engineering Journal 70 (1998) 115–124.
[17] A.J. Cessna, R. Grover, Journal of Agricultural and Food Chemistry 26 (1978) 289.
[18] M. Trillas, J. Peral, X. Doménech, Applied Catalysis B 3 (1993) 45.
[19] C. Kormann, D.W. Bahnemann, M.R. Hoffmann, Environmental Science and Technology 25 (1991) 494.
[20] S. Sakthivel, B. Neppolian, M.V. Shankar, B. Arabindoo, M. Palanichamy, V. Murugesan, Solar Energy Materials and Solar Cells 77 (2003).
[21] H.K. Singh, M. Saquib, M. Haque, M. Muneera, D. Bahnemann, Journal of Molecular Catalysis A: Chemical 264 (2007) 66–72.
[22] S. Malato, J. Blanco, M. Maldonado, P. Fernández-Ibanez, A. Campos, Applied Catalysis B: Environmental 28 (2000) 163–174.
[23] I. Poulios, E. Micropoulou, R. Panou, E. Kostopoulou, Applied Catalysis B: Environmental 41 (2003) 345–355.
[24] S. Malato, P. Fernández-Ibanez, M.I. Maldonado, J. Blanco, W. Gernjak, Catalysis Today 147 (2009) 1–59.
[25] S. Malato, J. Blanco, C. Richter, B. Milow, M.I. Maldonado, Water Science and Technology 40 (4–5) (1999) 123.
[26] C. Guillard, E. Puzenat, H. Lachheb, A. Houas, J.M. Herrmann, International Journal of Photoenergy 7 (2005) 1–9.
[27] R.A. Burns, J.C. Crittenden, D.W. Hand, V.H. Selzer, L.L. Sutter, S.R. Salman, Journal of Environment Engineering 125 (1999) 77–85.
[28] W.F. Jardim, S.G. Moraes, M.M.K. Takiyama, Water Research 31 (1997) 1728–1732.